Journal of Information Hiding and Multimedia Signal Processing ©2014 ISSN 2073-4212
Ubiquitous International Volume **5**, Number **4**, October **2014**

No-reference Quality Metric of Blocking Artifacts Based on Orthogonal Moments

Wei Zhang[1], Leida Li[1,2], Hancheng Zhu[1], Deqiang Cheng[1,*]

[1]School of Information and Electrical Engineering
China University of Mining and Technology
Xuzhou 221116, China

[2]Shanghai Key Laboratory of
Integrate Administration Technologies for Information Security
Shanghai 200240, China
*Corresponding author: iqacheng@163.com

Shu-Chuan Chu, John F. Roddick

School of Computer Science, Engineering and Mathematics
Flinders University of South Australia
South Australia 5001, Australia

Received November 2013; revised May 2014

Abstract. *This paper presents a no-reference quality metric for evaluating the blocking artifacts in images. It is based on a finding that the blocking artifact has direct effect on the distribution of discrete Tchebichef moments. The image is first divided into target blocks that cover potential artifacts. Tchebichef moments are then extracted as the block features. A local artifact score is computed by comparing the coefficients of the moments and the overall quality metric is obtained by taking the average of local estimates. Simulation results and comparisons demonstrate the advantage of the method.*
Keywords: Image quality assessment, Blocking artifacts, Tchebichef moment

1. **Introduction.** Digital images are inevitably subject to various distortions during their acquisition, processing and transmission. Image quality assessment (IQA) aims to model the distortions and generate a scalar to measure the extent of degradation. Since human eyes are the ultimate receiver, IQA methods should measure the image quality objectively and keep consistent to the subjective ratings. According to the availability of the original image, IQA methods can be classified into full-reference (FR) method, reduced-reference (RR) method and no-reference (NR) method [1, 2]. Most of the existing methods are FR ones, where the original image is used as a reference [3, 4, 5]. While FR methods can achieve very high prediction accuracy, the original image is not always available in practice. By contrast, NR methods generate the quality score using the distorted image only, so they are more useful in quality-aware image applications.

Without a reference image at hand, NR methods are more challenging. The vast majority of NR IQA algorithms aim to evaluate specific distortion, such as blocking, blur and ringing. Blocking artifacts are mainly caused by block-DCT based coding, such as JPEG and MPEG. Bovik et al. propose a method in DCT domain [6]. The blocking artifacts are first modeled as a 2D step function. The artifacts visibility map is then estimated by oriented activities and the brightness of local background. Finally, a scalar is generated to predict the overall image quality. Wang et al. evaluate both blocking and

blur in JPEG images [7]. Blocking artifacts are evaluated using the average difference across block boundaries, and blur is estimated by further combining intra-block activity. Perra et al. extract image edges using the Sobel operator. The luminance variations of both block boundary pixels and inner block pixels are calculated to produce the blockiness score [8]. Pan et al. propose an edge direction based blocking artifact metric [9]. It is based on the finding that when blocking artifacts appear, the directions of the block boundaries concentrate on 0° and 90°. The quality score is obtained based on the edge direction histogram. In [10], the difference image is processed along each row and column, producing one-dimensional signals. Then discrete Fourier transform is adopted to analyze the periodic peaks, which are signs of blocking artifacts. More recently, Lee et al. propose a method in spatial domain [11]. The candidate block boundaries are first determined using the pixel gradient across the block boundary. The boundaries with actual blocking artifacts are detected by investigating the pixel gradient values on both sides of the block boundary. The final quality score is computed as log of average strength of blockiness over the entire image. Although great achievements have been obtained in the literature, no-reference quality metrics of blocking artifacts are still demanding.

Orthogonal moment is efficient in image representation, and has been widely used in pattern recognition [12]. This motivates us to design NR IQA method using orthogonal moments. To this end, we propose a novel discrete Tchebichef moment based NR method for evaluating the blocking artifacts in images. It is based on our finding that blocking artifacts have direct effect on the distribution of the Tchebichef moments. The test image is first divided into target blocks in both horizontal and vertical directions, covering potential blocking boundaries. The quality score of the image is computed based on analysis of the moment features. The performance of the proposed method is demonstrated by experiments and comparisons. To the authors' knowledge, orthogonal moment based no-reference quality metric for blocking artifacts has rarely been addressed before.

2. **Discrete Tchebichef Moment.** The proposed method is based on discrete Tchebichef moment (TM) [13]. For an image $f(x, y)$ with size $M \times N$, the Tchebichef moments can be computed by projecting it onto a set of Tchebichef kernels $\{t_n(x)\}$:

$$T_{mn} = \frac{1}{\rho(m, M)\rho(n, N)} \sum_{x=0}^{M-1} \sum_{y=0}^{N-1} t_m(x) t_n(y) f(x, y), \tag{1}$$

where $\rho(n, N) = \sum_{x=0}^{N-1} \{t_n(x)\}^2$, $(m + n)$ is the order of the moment, $m = 0, 1, \cdots, M - 1, n = 0, 1, \cdots, N - 1$. The Tchebichef kernels satisfy the following orthogonal condition:

$$\sum_{x=0}^{N-1} t_m(x) t_n(x) = \rho(n, N)\delta_{mn}. \tag{2}$$

Due to the orthogonal property of TMs, the image can be represented using TMs as follows:

$$f(x, y) = \sum_{m=0}^{M-1} \sum_{n=0}^{N-1} t_m(x) t_n(y) T_{mn}. \tag{3}$$

TM is efficient in image representation, and has been widely used in visual pattern recognition, object classification and watermarking. For more details about TMs, the readers are kindly referred to [13].

3. **Proposed Method.** The proposed method is based on our finding that the strength of blocking artifact has direct effect on the distribution of TMs. Therefore, the proposed blocking artifact metric is defined by analyzing the distribution of the TMs.

3.1. **Target Block.** Blocking artifact is mainly caused by block DCT-based lossy coding, for example, JPEG compression. In JPEG, the image blocks (8×8) are quantized independently, and blocking artifact occurs right on the block boundaries. In order to evaluate the blocking artifacts, the target blocks that cover the block boundaries are first determined. As illustrated in Fig.1, A, B, C and D are four adjacent 8×8 blocks, which are exactly same to those used in JPEG compression. Blocking artifacts may occur at the boundaries of them, which are marked by thick lines. In order to evaluate the blocking, the target blocks should cover these boundaries. The two gray blocks in the figure show how the target blocks are determined. For blocks A and B, the target block covers the right half of A and the left half of B. For blocks A and C, the target block covers the bottom half of A and the upper half of C. It is easy to know that for an $M \times N$ image, the number of horizontal target blocks is $N_h = \lfloor M/8 \rfloor \times (\lfloor N/8 \rfloor - 1)$, and the number of vertical ones is $N_v = (\lfloor M/8 \rfloor - 1) \times \lfloor N/8 \rfloor$. The target blocks cover the potential blocking artifacts so that image quality can be evaluated based on them.

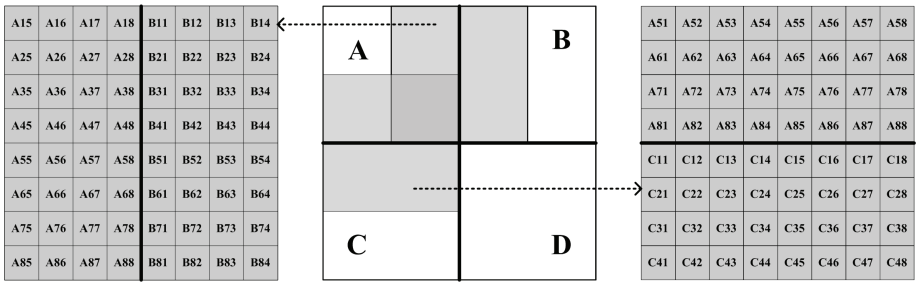

FIGURE 1. Method to obtain the target blocks.

3.2. **Effect of Blocking Artifact on TMs.** Blocking artifact has direct effect on the distribution of TMs. Fig.2 shows some target blocks with horizontal or vertical blocking artifacts, together with the energy distributions of TMs (14th order, $m = n = 7$). Note that the first and third images in the first row of the figure are taken from real images and magnified by 16 times for better display. The first and third images in the second row are generated using Matlab functions to simulate the ideal blocking artifacts.

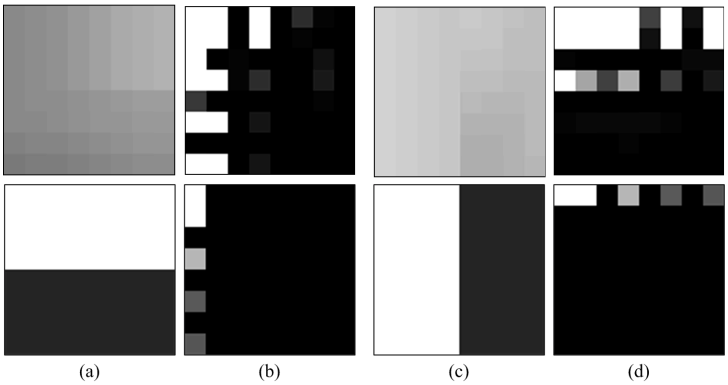

FIGURE 2. Target blocks with blocking artifacts and energy distribution of the Tchebichef moments. (a) Horizontal blocking artifact, (b) Energy map of (a), (c) Vertical blocking artifact, (d) Energy map of (c).

It is known from the figure that for the target block with horizontal blocking artifact, the energy map concentrates on the left half. Similarly, for vertical blocking artifact, the

energy map concentrates on the upper half. Furthermore, if the blocking artifact becomes more severe, the high energy coefficients will be more concentrated on the first row or first column. Based on this finding, we propose the following NR quality metric.

3.3. **Blocking Artifact Measure.** The proposed method operates in a local-to-global manner. This means the quality score of each target block is first obtained, and the global score is then generated by taking the average of local scores.

For a test image, the target blocks are first obtained. Since most DCT based coding systems use 8×8 blocks, the size of the target block is also 8×8. In implementation, the horizontal blocks with vertical artifacts are denoted by $\{B_k^H, k = 1, 2, \cdots, N_h\}$, while vertical blocks with horizontal artifacts are denoted by $\{B_k^V, k = 1, 2, \cdots, N_v\}$. For a target block, we first compute the $(m + n)$th order TMs, producing $(m + 1) \times (n + 1)$ moment coefficients:

$$T = \begin{pmatrix} t_{00} & t_{01} & \cdots & t_{0n} \\ t_{10} & t_{11} & \cdots & t_{1n} \\ \vdots & \vdots & \ddots & \vdots \\ t_{m0} & t_{m1} & \cdots & t_{mn} \end{pmatrix} \tag{4}$$

For $B_k^H, k = 1, 2, \cdots, N_h$, the sum of absolute moment coefficients at the bottom half is first computed. Then the local quality score is obtained by computing the ratio of this sum to that of all absolute moment coefficients (without $|t_{00}|$):

$$Q_k^H = \frac{\sum_{i=\lfloor \frac{m+1}{2} \rfloor}^{m} \sum_{j=0}^{n} |t_{ij}|}{\left(\sum_{i=0}^{m} \sum_{j=0}^{n} |t_{ij}|\right) - |t_{00}|}, k = 1, 2, \cdots, N_h, \tag{5}$$

where $\lfloor \cdot \rfloor$ is the floor operation. Similarly, for $B_k^V, k = 1, 2, \cdots, N_v$, the local quality score is

$$Q_k^V = \frac{\sum_{i=0}^{m} \sum_{j=\lfloor \frac{n+1}{2} \rfloor}^{n} |t_{ij}|}{\left(\sum_{i=0}^{m} \sum_{j=0}^{n} |t_{ij}|\right) - |t_{00}|}, k = 1, 2, \cdots, N_v. \tag{6}$$

In Eqs.(5) and (6), $|t_{00}|$ is reduced from the denominator, because it denotes for the average gray value of the target and is not related to the blocking artifact.

After obtaining the quality scores for each target block in both horizontal and vertical directions, we compute the average of them. The scores of the horizontal blocks are denoted by $\{Q_k^H, k = 1, 2, \cdots, N_h\}$ and those of the vertical blocks are denoted by $\{Q_k^V, k = 1, 2, \cdots, N_v\}$. Then the average scores of horizontal blocks and vertical blocks are obtained by

$$Q^H = \frac{1}{N_h} \sum_{k=1}^{N_h} Q_k^H, Q^V = \frac{1}{N_v} \sum_{k=1}^{N_v} Q_k^V. \tag{7}$$

Finally, the blocking artifact score of the whole image is obtained:

$$Q = \frac{Q^H + Q^V}{2}. \tag{8}$$

It is easy to know that the proposed quality metric has the range (0, 1). A quality score approaching zero indicates that the blocking artifact in the image is severe, while a score approaching one shows that the image quality is good without apparent blocking artifacts.

4. **Experimental Results.** Blocking artifact is the main source of degradation for JPEG compressed images. In this part, the performance of the proposed method is evaluated on JPEG images from two pubic databases, including LIVE [3, 14] and MICT [15]. The LIVE database contains 175 JPEG compressed images, together with 58 uncompressed images which are also used to evaluate the performance of the proposed method. The subjective quality of this database is measured using Differential Mean Opinion Score (DMOS). The MICT database contains 98 JPEG images, and the subjective quality is measured using Mean Opinion Score (MOS). In simulations, the order of Tchebichef moment is 14 ($m = n = 7$).

Fig.3 shows some of the JPEG images from LIVE database and their quality scores. For reference, the bit rates of the images are also provided. It is known from the figure that when the bit rate decreases, the blocking artifact becomes more obvious and the quality score decreases accordingly. Another interesting finding is that when the bit rates are similar, the quality scores are approximately the same.

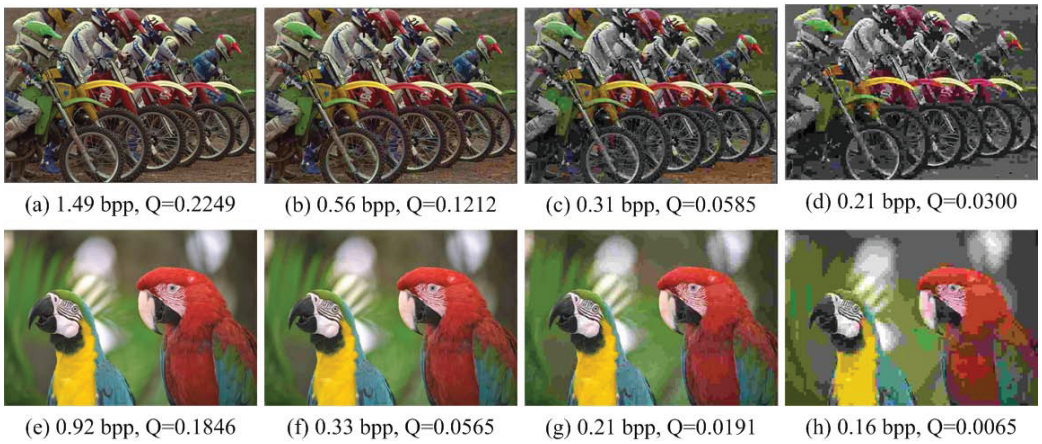

FIGURE 3. Distorted images and their quality scores.

In order to evaluate the performance of the method, the following four-parameter nonlinear mapping is conducted between the predicted scores and the subjective ratings:

$$f(x) = \frac{\tau_1 - \tau_2}{1 + e^{(x-\tau_3)/\tau_4}} + \tau_2, \tag{9}$$

where $\tau_1, \tau_2, \tau_3, \tau_4$ are determined automatically so that the difference between the objective scores and the subjective ratings is minimized. Based on the nonlinear fitting, Pearson correlation coefficient (CC) and the root mean-squared error (RMSE) are computed to evaluate the predication accuracy. Spearman rank-order correlation coefficient (SROCC) is employed to evaluate the monotonicity.

Fig.4 shows the scatter plots between DMOS and the predicted scores on LIVE for the proposed method and four other no-reference blocking artifact metrics. It can be seen that the predicted scores correlate well with subject ratings. Based on these fittings, CC, RMSE and SROCC are computed to estimate the performance of the methods. The simulation results are listed in Table 1 and Table 2.

It is known from Table 1 that the proposed algorithm achieves the highest accuracy for LIVE database. CC is the highest and RMSE is the lowest. Lee's method is comparable to our method with slightly lower CC and slightly better SROCC.

The experimental results in Table 2 indicate that the proposed method outperforms the other algorithms significantly. Pan's method and Chen's method achieve comparable results in this database. Perra's and Lee's methods produce unsatisfactory results on this

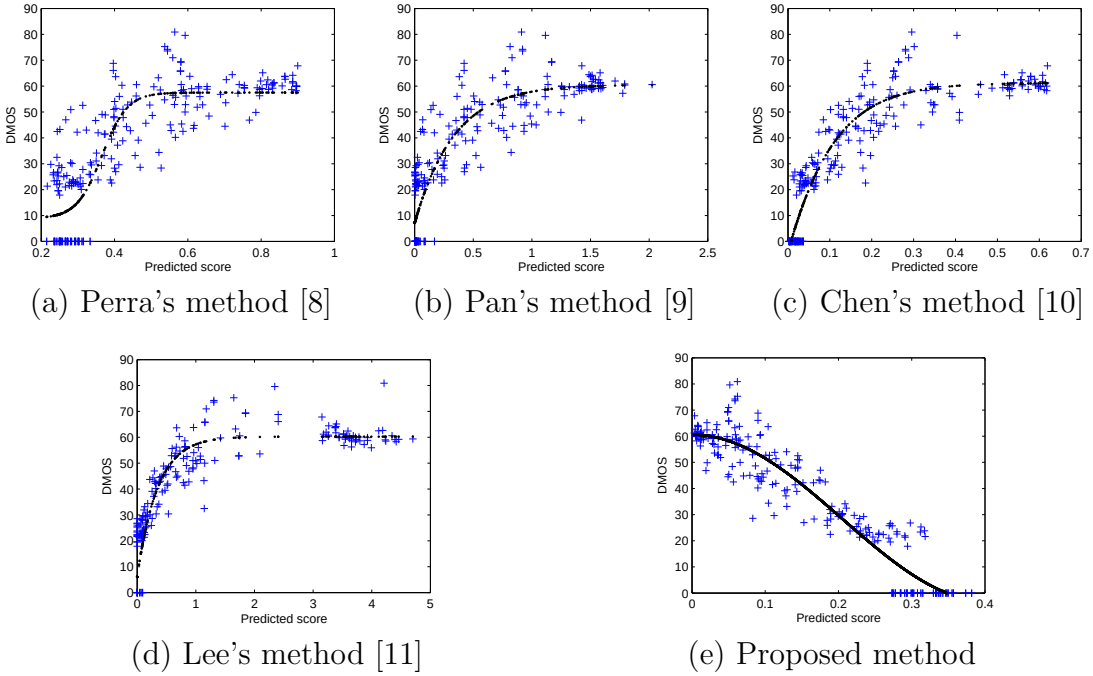

(a) Perra's method [8] (b) Pan's method [9] (c) Chen's method [10]

(d) Lee's method [11] (e) Proposed method

FIGURE 4. Scatter plots between DMOS and predicted scores on LIVE database.

TABLE 1. Simulation results on LIVE database.

Metric	CC	RMSE	SROCC
Perra [8]	0.8570	12.5003	0.8268
Pan [9]	0.8887	11.1252	0.8728
Chen [10]	0.9356	8.5237	0.9193
Lee [11]	0.9426	8.0976	**0.9296**
Proposed	**0.9447**	**7.9528**	0.9225

TABLE 2. Simulation results on MICT database.

Metric	CC	RMSE	SROCC
Perra [8]	0.7993	0.7930	0.7517
Pan [9]	0.8350	0.7260	0.8253
Chen [10]	0.8381	0.7198	0.8228
Lee [11]	0.7625	0.8538	0.8097
Proposed	**0.9087**	**0.5509**	**0.8916**

database. By comparison, the proposed method performs consistently well on both LIVE and MICT databases.

Fig.5 shows the relation between the predicted scores (Q) and the bit rate (bpp) for the 175 JPEG images. In the figure, each triangle corresponds to an image. It is well-known that when the bit rate is small, the compression is severe and more blocking artifacts may appear. It is observed that the quality score increases when the bit rate gets higher. This figure also demonstrates that the proposed method achieves good monotonicity.

While promising results have been obtained using the proposed method, a possible deficiency of our method is that it cannot differentiate between high quality images and images with apparent blocking artifacts. This can be seen from Fig.4(f). In the figure,

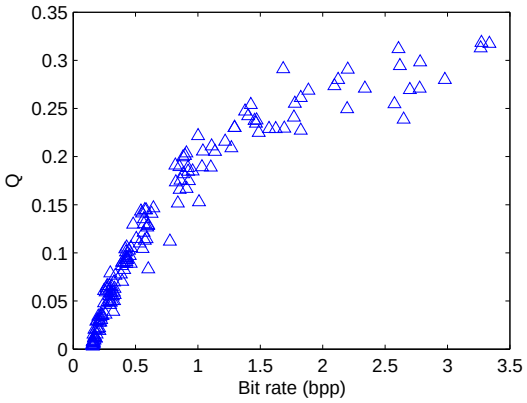

FIGURE 5. Plot of Q versus bit rate (bpp).

while the predicted scores of the high quality images (DMOS=0, without visible blocking artifacts) are high, they are indeed different. This also indicates that further improvement is needed. This can be done by incorporating the characteristics of Human Visual System (HVS). In other words, the presence of blocking artifacts should be determined before computing the quality score. In this way, the high quality images can be assigned a constant score, and the evaluation can be conducted only on the blocks/images with visible artifacts.

5. **Conclusion.** In this paper, we propose a novel no-reference image quality assessment method to evaluate the blocking artifacts in images. The main contribution of this work is the utilization of discrete Tchebichef moments in designing the blocking metric. Particularly, the inherent relation between the blocking artifact and the distribution of the moments is discovered. Our method is efficient in predicting the blocking artifacts in images, and it even outperforms some of the popular full-reference quality metrics. While promising results have been obtained, we also find that our method produces unsatisfactory results for high quality images (without visible blocking artifacts). Our ongoing work is to solve this problem by incorporating the characteristics of HVS.

The proposed method operates in a local-to-global manner, which means the strength of blocking artifact can be estimated at a block level or an image level. This may be useful for some image applications, such as image deblocking and image forensics. For image deblocking, the local blocking score can be generated and facilitate adaptive deblocking algorithms. In image forensics, the discrepancy of local blocking artifacts can be a sign of image forgery. Incorporating the proposed method into these researches will be an interesting topic.

Acknowledgments. This work is supported in part by National High-Tech R&D Program of China (863 Program, 2012AA062103), National Natural Science Foundation of China (61379143, 51204175, 51204176, U1261105), the Fundamental Research Funds for the Central Universities (2012QNA59), and the Opening Project of Shanghai Key Laboratory of Integrate Administration Technologies for Information Security (AGK2012002) and the S&T Program of Xuzhou City (XM13B119).

REFERENCES

[1] D.M. Chandler, Seven challenges in image quality assessment: past, present, and future research, *ISRN Signal Processing*, vol. 2013, pp. 1-53, 2013.

[2] W.S. Lin, and C.C. Jay Kuo, Perceptual visual quality metrics: a survey, *Journal of Visual Communication and Image Representation*, vol. 22, no. 4, pp. 297-312, 2011.
[3] Z. Wang, A.C. Bovik, H.R. Sheikh, and E.P. Simoncelli, Image quality assessment: from error visibility to structural similarity, *IEEE Trans. Image Processing*, vol. 13, no. 4, pp. 600-612, 2004.
[4] H.R. Sheikh, and A.C. Bovik, Image information and visual quality, *IEEE Trans. Image Processing*, vol. 15, no. 2, pp. 430-444, 2006.
[5] D.M. Chandler, and S.S. Hemami, VSNR: a wavelet based visual signal-to-noise ratio for natural images, *IEEE Trans. Image Processing*, vol. 16, no. 9, pp. 2284-2298, 2007.
[6] A.C. Bovik, S. Liu, DCT-domain blind measurement of blocking artifacts in DCT-coded images, *Proc. of IEEE International Conference on Acoustics, Speech, and Signal Processing*, pp. 1725-1728, 2001.
[7] Z. Wang, H.R. Sheikh, No-reference perceptual quality assessment of JPEG compressed images, *Proc. of IEEE International Conference on Image Processing*, pp. 477-480, 2002.
[8] C. Perra, F. Massidda, and D.D. Giusto, Image blockiness evaluation based on sobel operator, *Proc. of IEEE International Conference on Image Processing*, pp. 389-392, 2005.
[9] F. Pan, X. Lin, S. Rahardja, E.P. Ong, and W.S. Lin, Using edge direction information for measuring blocking artifacts of images, *Multidimensional Systems and Signal Processing*, vol. 18, no. 4, pp. 297-308, 2007.
[10] C. H. Chen, and J.A. Bloom, Image blockiness evaluation based on sobel operator, *Proc. of Pacific-Rim Conference on Advances in Multimedia Information Processing*, pp. 112-123, 2010.
[11] S.W. Lee, and S.J. Park, A new image quality assessment method to detect and measure strength of blocking artifacts, *Signal Processing: Image Communication*, vol. 27, no. 1, pp. 31-38, 2012.
[12] J. Flusser, T. Suk, and B. Zitová, *Moments and Moment Invariants in Pattern Recognition*, Wiley, Natick, MA, USA, 2009.
[13] R. Mukundan, S.H. Ong, and P.A. Lee, Image analysis by Tchebichef moments, *IEEE Trans. Image Processing*, vol. 10, no. 9, pp. 1357-1364, 2001.
[14] LIVE Image Quality Assessment Database Release 2, http://live.ece.utexas.edu/research/quality.
[15] MICT Image Quality Evaluation Database, http://mict.eng.u-toyama.ac.jp/mictdb.html.